Egypt.J.Chem. **Vol. 62**, Special Issue (Part 1), pp. 177 - 195 (2019)

Egyptian Journal of Chemistry
http://ejchem.journals.ekb.eg/

Efficient Removal of Oxytetracycline and Some Heavy Metals from Aqueous Solutions by Mg-Al Layered Double Hydroxide Nanomaterial

Mohamed E. M. Hassouna[1]*, Ragab R. Amin[2], Alaa A. Ahmed-Anwar[3] and Rehab K. Mahmoud[1]

[1]*Chemistry Department, Faculty of Science,62514 Beni-Suef University, Beni-Suef , Egypt.*
[2]*Basic Science Department, Faculty of Engineering, Nahda University, Beni-Suef, Egypt.*
[3]*Analytical Chemistry Department, Central Research Laboratory, Nahda University, Egypt.*

THE development of an efficient method for the removal of oxytetracycline and some heavy metals from aqueous solutions by Mg-Al layered double hydroxide nanomaterial. Preparation and characterization of [Mg-Al]-LDH and its evaluation for the removal of Cu^{2+}, Ni^{2+}, Co^{2+}, Zn^{2+}, Fe^{2+} and oxytetracycline from aqueous solutions. Water contamination by antibiotic contaminants and heavy metal ions represents an important environmental remediation problem. Oxytetracycline is an antibacterial drug used for human, fish, plants and animals' treatment, so it is found in large concentrations in wastewater. Mg–Al LDH nanoparticles with nitrate intercalated anions, as an adsorbent, was prepared through coprecipitation technique of solutions of magnesium nitrate hexahydrates and aluminum nitrate (with percentage 3:1 molar ratio respectively). The nanomaterial was characterized before and after adsorption of some pollutants in wastewater by X-ray diffraction (XRD), Fourier transform infrared (FTIR) surface area analysis (BET), field emission scanning electron microscopy (FESEM) high resolution transmission electron microscopy (HRTEM), Various factors such as pH (3-10), dose of Mg-Al LDH (0.025-0.2g), concentration of metal ions (15-60 ppm) and effect of shaking time (5-120 min) were applied to optimize the removal ability of Mg-Al LDH. The adsorption efficiency of the pollutant by Mg-Al LDH was calculated, the kinetics and the isotherm of adsorption strength over the adsorbent were further studied. The adsorption capability of the adsorbent was studied with regard to several pollutants in wastewater like (copper, zinc, iron, cobalt, nickel metal ions and oxytetracycline) in single solution.

Keywords: Mg–Al LDH nanoparticles, Adsorption removal, Heavy metals (copper, zinc, iron, cobalt, nickel), Oxytetracycline

Introduction

Increasing worldwide contamination of fresh water systems has become one of the key environmental problems facing humanity; Oxytetracycline used in fish farming industry to treat bacterial diseases [1]. It is found in water in high concentrations so it is considered as an important water pollutant. Water contamination by antibiotic contaminants and heavy metal ions represents an important environmental remediation problem [2]. In some cases, these pollutants interact with each other's in wastewater producing more toxic substances and more contamination problems are generated[3]. Hence, the critical need for efficient techniques to remove these harmful pollutants[4-7].

Residues of antibiotics have been detected in water resources that receive effluents of wastewater treatment plants, agriculture run off and discharges of pharmaceutical manufacturers [8-10]. The presence of low levels of antibiotics and their transformation products in the environment cause the spread of antibiotics' resistance bacteria which clearly shows that the elimination in sewage treatment plants is often incomplete[2]. Oxytetracycline is an antibacterial drug used for human, fish, plants and animals treatment, so it

*Corresponding author e-mail: mhassouna47@hotmail.com; mohamed.hassona@science.bsu.edu.eg
Fax: +20822334551
Received 6/11/2018; Accepted 15/6/2019
DOI: 10.21608/ejchem.2019.6102.1510

is found in large concentrations in wastewater. The United States data on used antimicrobials for treatment of bacteria disease of plants are limited to streptomycin and oxytetracycline [11]. The presence of high levels of oxytetracycline in water and when translocate to plants is harmful to human life. Rats that were given combinations of aminopyrine or oxytetracycline and sodium nitrite in drinking water, after feeding a dose of (0.1 %) (1, 000ppm) of oxytetracycline and sodium nitrite for 60 weeks, liver tumors picked off 4 of 30 rats (3 hepatocellular tumors and 1 cholangioma)[3]. The reason for which the presence of oxytetracycline in water has had the same impact known for the contamination of water with some metal ions and their assured risk on the environment. The immediate importance is the toxicity of these compounds to aquatic organisms and human through drinking of contaminated water or eating vegetables and crops irrigated by it [12-14].

Various materials such as activated carbon [5, 15-18], biomaterials[19], polymers[20], and sorption resins[21] have been used for adsorption of metal ions. Most of these methods have low selectivity and weak affinity for heavy metal ions[22]

LDH material has excellent selectivity for removal of heavy metal ions [23]. Also, many physical techniques such as electro dialysis, crystallization, reverse osmosis, are available for the same purpose, but such techniques are of high cost [24, 25].

Several adsorbents such as chicken bone-based biochar [26], multi-walled carbon nanotubes[27], layered carbon particles prepared from seaweed biomas[28] and rice husk ash [29] have been described for the removal of tetracycline from different wastewaters. Recently, [30] $CoO/CuFe_2O_4$ mixed metal oxide has been synthesized from layered double hydroxides for tetracycline removal from industrial wastewater. Emerging pharmaceuticals from wastewater have been removed by ozone-based advanced oxidation processes [31]. Layered double hydroxides (LDHs) have drawn considerable attention for their use in the removal of pollutants (such as heavy metal ions) due to their high removal efficiency and environmental friendliness.[32, 33]. LDHs have proven to be good candidates for removing antibiotics from aqueous solutions [34]. These materials, which are endowed with high anionic exchange capacity and good adsorption ability, have been able to retain and host several large organic anions [35], cations [36], dyestuff [37-41] and are used for water remediation [42] . The anion exchange adsorption using diverse adsorbents has attained special importance; such studies which use LDH are quiet scarce [43-46]. LDH compounds have unique characteristics such as low cytotoxicity, good biocompatibility, controllable particle sizes, varied functionality, high loading capacity, wide availability and the protection of biomolecules in interlayers [47]

LDHs are 2D materials recognized as potential resources for therapeutic and imaging purposes owing to their biocompatibility and low toxicity, among other properties essential to Nano medicine [48].

LDHs, also called hydrotalcite-like compounds and anionic clays, are based on the brucite, $Mg(OH)_2$, layers with partial substitution of trivalent or divalent cations [49, 50]. The net positive charge is then balanced by exchangeable hydrated anions [51] .

The present work focuses on the preparation and characterization of [Mg-Al]-LDH and its evaluation for the removal of Cu^{2+}, Ni^{2+}, Co^{2+}, Zn^{2+} Fe^{2+} and oxytetracycline from aqueous solutions. Besides, understanding the mechanism of interaction between the adsorbent and adsorbates for an eventual use of the system to remove such inorganic and organic pollutants and allows for fine control of the composition of the LDH.

Materials and Methods

Chemicals

Magnesium nitrate hexahydrates ($Mg(NO_3)_2.6H_2O$), aluminum nitrate ($Al(NO_3)_3$), sodium hydroxide (NaOH), copper sulphate ($CuSO_4$), nickel sulphate ($NiSO_4$), cobalt chloride ($CoCl_2$), ferrous chloride ($FeCl_2$), zinc sulphate ($ZnSO_4$) and oxytetracycline ($C_{22}H_{24}N_2O_9$), as starting chemicals. All used chemicals were of analytical grade and were not more purified and used solutions during the experiments were freshly prepared in deionized water obtained from selected HP (High Purity) water system.

Preparation of Mg-Al layered double hydroxide

The Mg-Al nitrate LDH was prepared by blending a mixture of magnesium nitrate and aluminum nitrate (3: 1 molar ratio respectively) Fig.1. 2M of sodium hydroxide was then added drop by drop with stirring at 60°C till pH 10, then heating was stopped and stirring was continued

for 24 hours. The precipitate was filtered and washed with deionized water many times. Then the precipitate was dried at 80°C

Characterization.

X-ray diffraction experiments were conducted on a PANalytical (Empyrean) FT-IR. FT-IRaman spectra were recorded with a Bruker (Vertex 70 FTIR-FT Raman Massachusetts 01821, United States of America) spectrometer. The microstructures of the adsorbents were examined by high-resolution transmission electron microscopy (HRTEM, JEOL-JEM 2100), and the morphologies were characterized using field emission scanning electron microscopy (FESEM). The BET specific surface area, specific pore volume, and pore sizes of the adsorbent materials were determined by N_2 adsorption isotherms using an automatic surface analyzer (TriStar II 3020, Micromeritics, USA). Particle sizes and zeta potentials were determined on a Malvern instrument (Malvern Instruments Ltd). (Quanta FEG250) took EDAX.

Heavy metals and oxytetracycline adsorption study

Heavy metal ions (Cu^{2+}, Ni^{2+}, Co^{2+}, Zn^{2+}, Fe^{2+}) or oxytetracycline batch adsorption process were studied at ambient temperature using 50 mL of the pollutant solution in 250 mL conical flask and shaking at speed of 200 rpm using orbital shaker. Different parameters such as pH (3-10), dose of adsorbent (0.025, 0.05, 0.15, 0.1, 0.2), initial pollutant concentration (15-60 ppm) and time (5-120 min) were applied. The pH was adjusted using 0.1 M HCl and 0.1 M NaOH and measured by (A ∂wa – AD1030) pH meter. (Cu^{2+}, Ni^{2+}, Co^{2+}, Zn^{2+}, Fe^{2+}) concentrations were quantified using atomic absorption spectrophotometer (model ZEISS-AA55, Germany), while the absorbance of the aqueous solution of oxytetracycline has been measured at λ_{max} equals to 275 nm, against deionized water as a blank using UV-VIZ (Shimadzu 1800 UV). The removal percent and the quantity adsorbed of heavy metal ions and oxytetracycline by the Mg-Al LDH were calculated as shown in the following equations:

$$Removal\,\% = \frac{(C_o - C_{eq})}{C_o} \times 100 \qquad (1)$$

$$q_e = \frac{(Co - Ceq)V}{m} \qquad (2)$$

Where C_o, C_{eq} are the initial and equilibrium concentrations, q_e (mg/g) is the quantity adsorbed. V, corresponding to heavy metals and oxytetracycline-solution volume. m, is the mass of the adsorbent.

The adsorption isotherms

Were operated by dispersing 50 mg Mg-Al LDH in 50 mL (Cu^{2+}, Ni^{2+}, Co^{2+}, Zn^{2+}, Fe^{2+} and oxytetracycline) solutions at different concentrations varying from 15 to 60 mg L^{-1}.

The adsorption of (Cu^{2+}, Ni^{2+}, Co^{2+}, Zn^{2+}, Fe^{2+} and oxytetracycline) on Mg-Al LDH was undertaken by mixing 50 mg of adsorbent with 50 mL of 20 mg L^{-1} of each of (Cu^{2+}, Ni^{2+}, Co^{2+}, Zn^{2+}, Fe^{2+} and oxytetracycline) solution.The adsorption isotherm have been developed for evaluating the equilibrium adsorption of compounds from solutions by two equilibrium models *viz.,* Langmuir and Freundlich models (52):

$$\frac{C_e}{q_e} = \frac{1}{(q_o K_L)} + \frac{1}{(q_o)} C_e \qquad (3)$$

$$\ln q_e = \ln K_F + (\frac{1}{n}) \ln C_e \qquad (4)$$

In the kinetic study

Kinetic models have been applied for studying the rate-controlling mechanism like: mass transfer, chemical reaction and diffusion control. To examine the mechanisms of the pollutant adsorption process, the pseudo-first-order model suggested that the binding generated from physical adsorption can be interpreted by equation 5. The pseudo second-order model is rooted in chemical adsorption (chemisorption) and can be presented by equation 6. In addition, the kinetic results are analysed, using the intraparticle diffusion model to explain the diffusion mechanism. This model is representeded in equation 7 through:

$$\ln(q_{e-} q_t) = \ln(q_e) - k_1 t \qquad (5)$$

$$\frac{t}{q} = \frac{1}{k_2 q_e^2} + \frac{t}{q_e} \qquad (6)$$

$$q_t = k_i t^{0.5} + C \qquad (7)$$

Where q_t and q_e are considered the amounts of Cu^{2+} adsorbed on the LDH adsorbent in mg (adsorbate)/g (adsorbent) at time t and at equilibrium, respectively, k_1 is regarded as the rate constant of the pseudo first-order model (min^{-1}). The values of q_e and k_1 are calculated

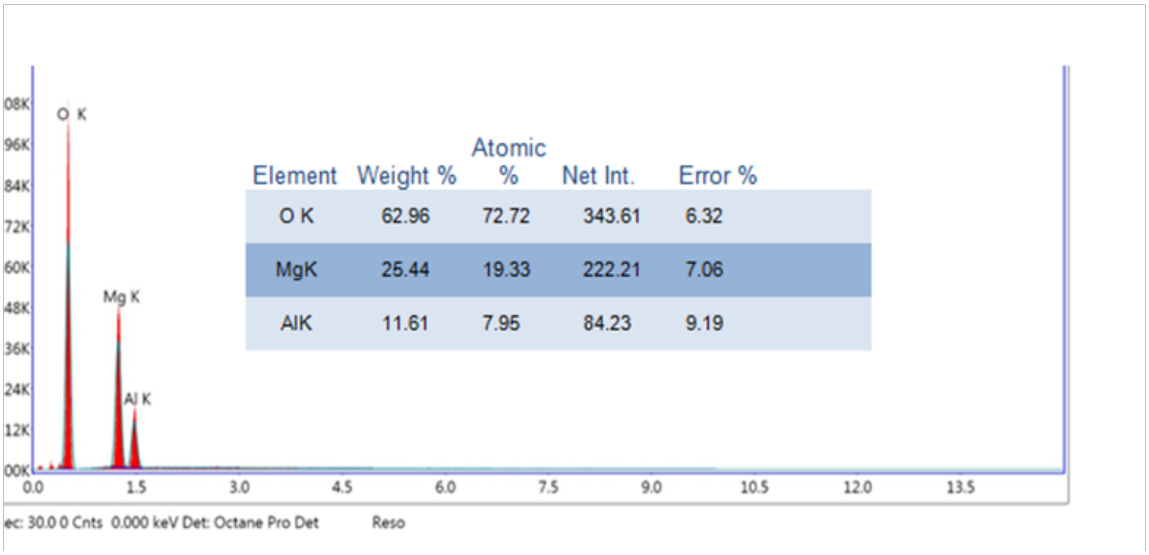

Fig. 1. EDAX of Mg-Al Layered double hydroxide.

from the intercept and the slope of the linear plot of ln $(q_e - q_t)$ versus t. K_2 is the rate constant of the pseudo second-order model (g/mg min). The slope and intercept of the linear plot of t/q_t against t yielded the values of q_e and k_2. Finally C is the intercept and k_i is the intraparticle diffusion rate constant (mg/g $min^{1/2}$) which was determined by the slope of the linear plot of q versus $t^{0.5}$. The experiment was repeated three times and the average values were reported.

Results and Discussion

For convenience, the different parameters will be separately discussed.

Characterization

The FT-IR spectrum was investigated to estimate the structure of the Mg-Al LDH, before and after adsorption of oxytetracycline as a representative example as shown in Fig. 2. The chemical bonds in the Mg-Al- NO_3 LDH were identified by the band that is centered at 590 cm^{-1} which was attributed to M–O–M vibration [53-55], this band like the M–O–H bending [55], involves the oxygen metal ions translational motion in the brucite-like layers [56, 57]. The strong broad band at 3487 cm^{-1} was related to the stretching vibrations of the H-bond of the OH group (ν O–H) in the brucite-like layers [54, 58] .The bending vibration (δ H_2O) of the H_2O molecules in the interlayers [57] appeared at 1644 cm^{-1}. The peak located at 1383 cm^{-1} was related to the ν_3 extending vibration of the NO_3 groups in the LDH interlayer. The FT-IR spectrum of Mg-Al LDH before and after adsorption indicated that comparable peaks and new ones corresponding to the drug (3430 and 1607cm^{-1}) were appeared for amide (NH_2) and carbonyl (C=O) groups respectively. The FTIR patterns (Fig. 2) showed that the adsorption peak of OH group shifted from 3487 cm^{-1} to 3430 cm^{-1} after oxytetracycline adsorption. In FTIR spectra (Fig. 2) confirming the successful adsorption of oxytetracycline on the LDH.

Fig.3. Shows the XRD patterns of Mg-Al LDH. The XRD confirmed the structure of the Mg-Al LDH compared to ICDD card no (00-048-0601) (58). Mg-Al LDH was indexed to the rhombohedral crystal structure with space group of R-3m and the unit cell parameters d-values (basal spacing) is (7.97 Å). The crystallite size is 81.77 nm. After adsorption of oxytetracycline the basal peak (003) position in the oxytetracycline-LDH corresponds to an interlayer distance of d-values is (7.71 Å) which is smaller than Mg-Al LDH by 0.26 Å where the structure is illustrated in Scheme.1, which means that oxytetracycline is adsorbed on the surface of LDH layers. All peaks of oxytetracycline –LDH showed the same diffraction peaks of the LDH confirming its stability structure after adsorption. The basal planes (003), (006) and the broadening of (015) and (018) planes confirmed the layered structure of LDH. No material has been contaminated by atmospheric CO_2 and also confirmed by the x-ray, as no peak corresponding to a carbonate intercalated

hydrotalcite-like phase was recorded.

Figure 4 describes the FESEM and the HRTEM micrograph images of the Mg-Al and Mg-Al oxytetracycline LDH. The Figures show that the microstructures of LDH samples were uniform in nature. The porous nanosheets of the prepared LDHs are observed in Fig. 4 (a, b, c, d). The images illustrate the nanosheets structures with a thickness of about 5-45 nm and are composed of plate-like nanoparticles.

The FESEM images of Mg-Al LDH, which support the results of the XRD, where the plate like morphology of LDH are appeared in the FESEM images which are shown in Fig.4 (a, b, c, d). The HRTEM micrographs further confirm the observations XRD (fig 4f & e). The HRTEM images displayed the layered structures in Fig.4 (e), (f); after drug's loading oxytetracycline on Mg-Al LDH, the layered structure appeared confirming that it is stable after the drug loading. The sectional area electron diffraction (SAED) pattern taken from individual planes revealed the crystallinity of LDHs.

The determination of zeta potential has important uses in water treatment field. It is a measure of the magnitude of the charge repulsion/ attraction between particles in solution, and is one of the main factors known to affect stability. Also, gives details about the causes of dispersion, or aggregation. As shown in Figure 5, zeta potentials for the size distributions intensity of Mg-Al LDH before and after adsorption with oxytetracycline were at (193.3) and (318.9) nm, respectively. Those of aqueous dispersions of the Mg-Al and Mg-Al oxytetracycline LDH were (8.31) and (-13, 3) mV, respectively as shown in table 1, at optimized pH 6.0. The results show that the positive zeta potential, which is related to the Mg-Al LDH nanomaterial is attributed to the interactions between the inorganic material and the organic pollutant such as oxytetracycline [55].

Figure (6) shows the N_2 adsorption–desorption isotherms and the pore-size distribution for the synthesized Mg-Al LDH. The Mg-Al LDH showed a small surface area of 4.0184 m^2g^{-1} which agrees with the FESEM due to a decrease of the nucleation rate and favored crystal growths of the

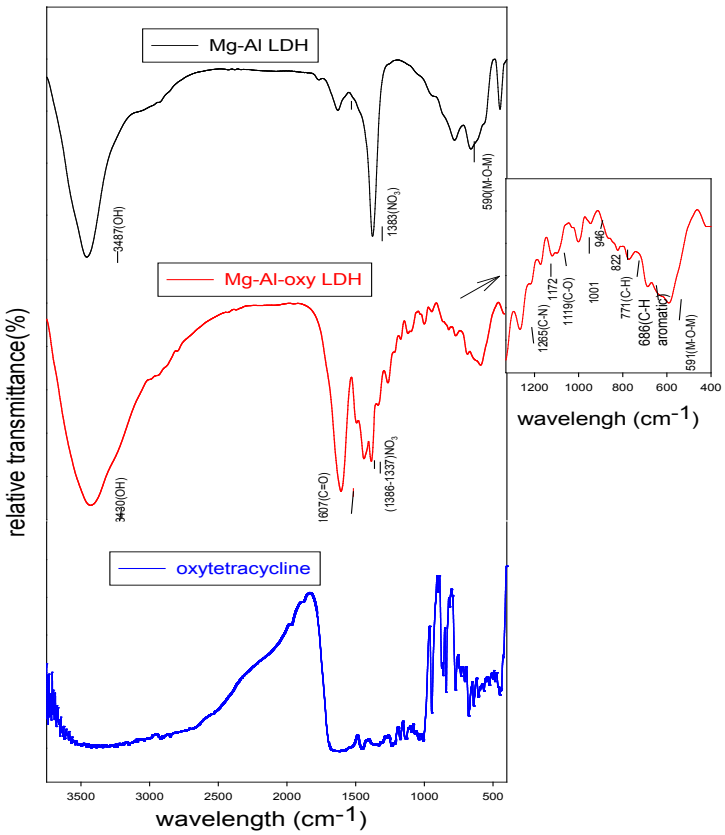

Fig. 2. FT-IR spectra of Mg-Al layered double hydroxide and Mg-Al/ Oxytetracycline LDH.

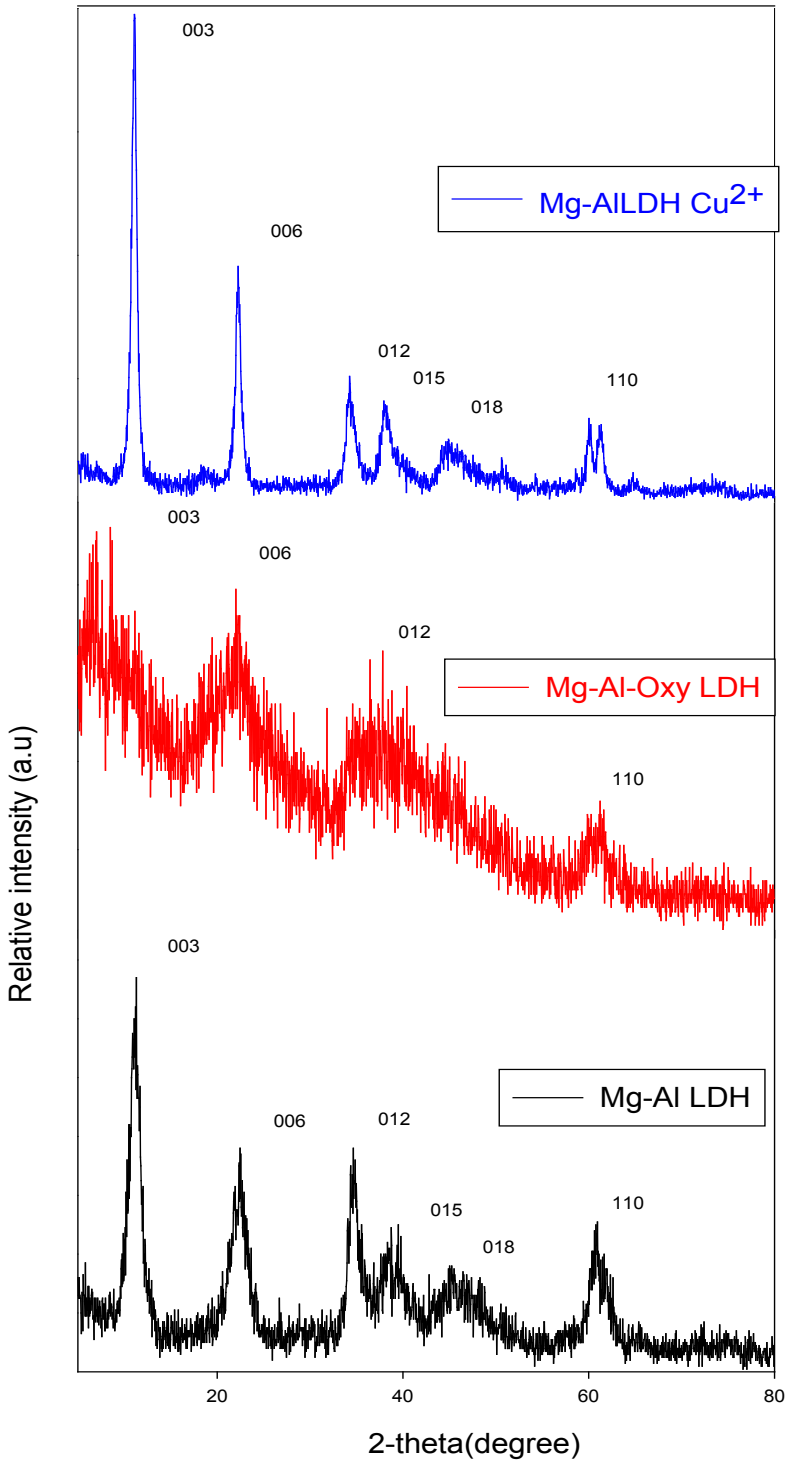

Fig. 3. XRD patterns of Mg Al LDH, Mg-Al LDH after adsorption of oxytetracycline and Cu 2+.

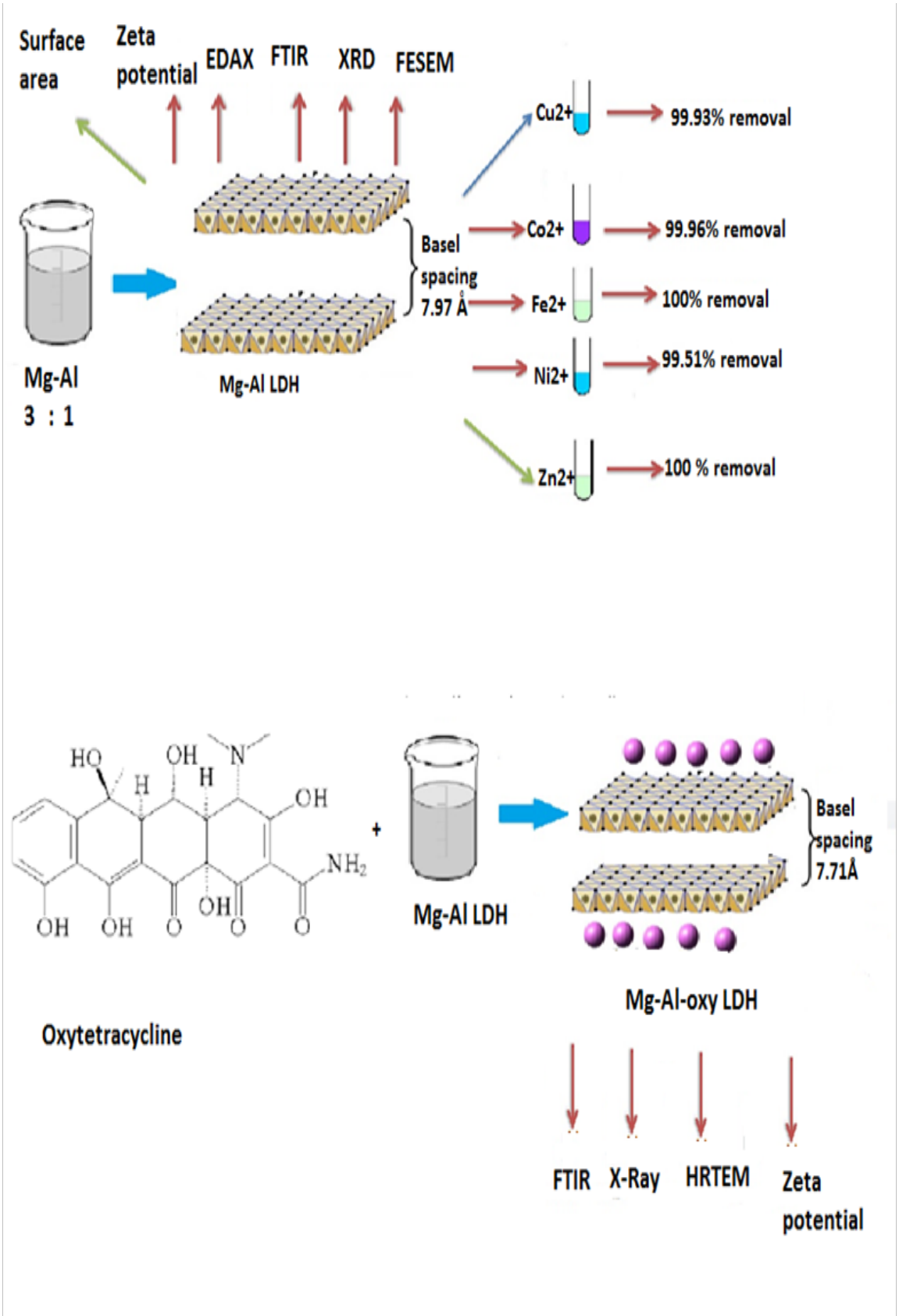

Scheme 1. Diagram shows the preparation steps of Mg-Al LDH, The adsorption mechanism of oxytetracycline on M-Al LDH.

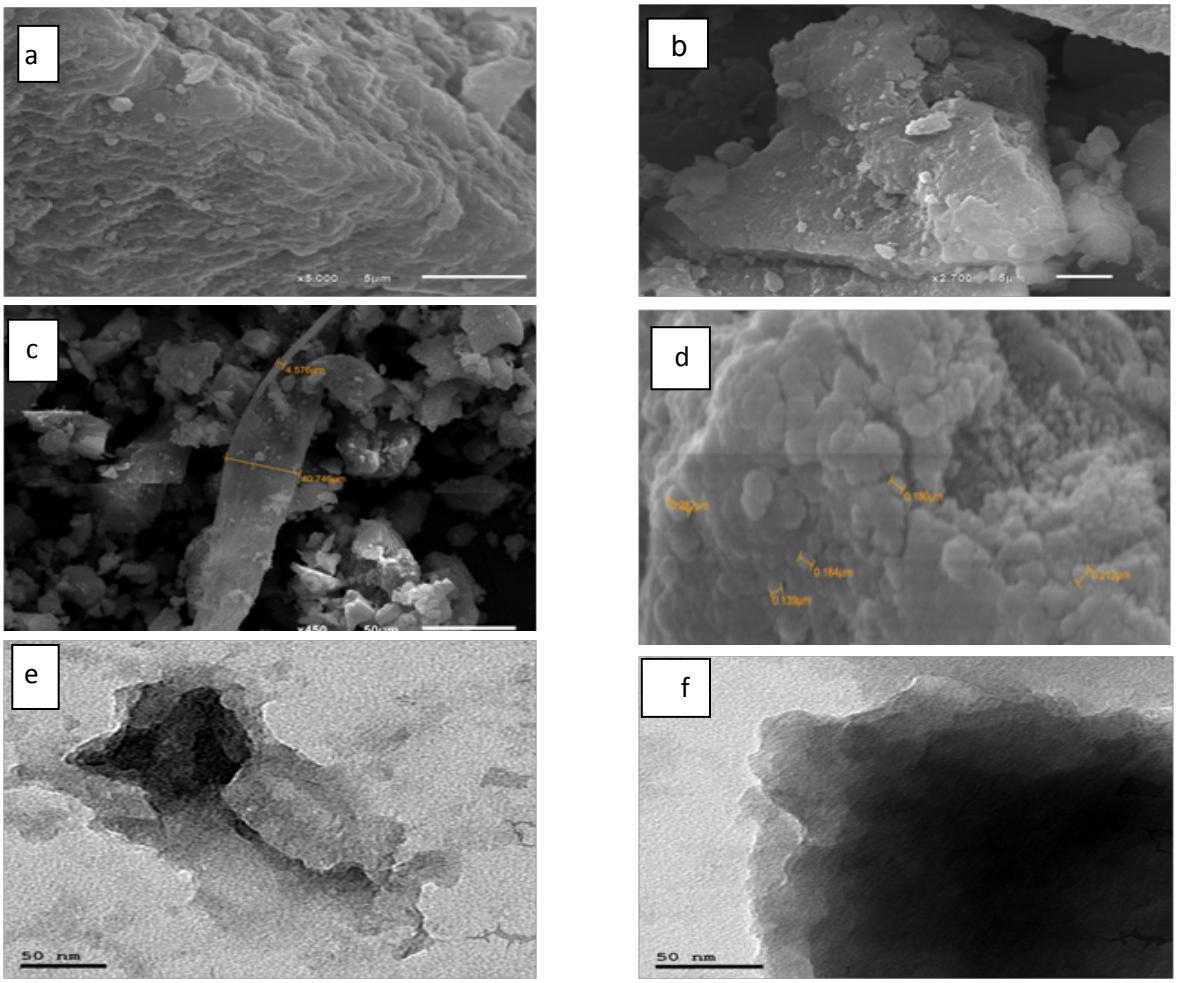

Fig.4. (a),(b),(c),(d) FESEM of Mg-Al LDH, (e),(f) HRTEM of Mg-Al LDH after adsorption of oxytetracycline on mg-Al LDH.

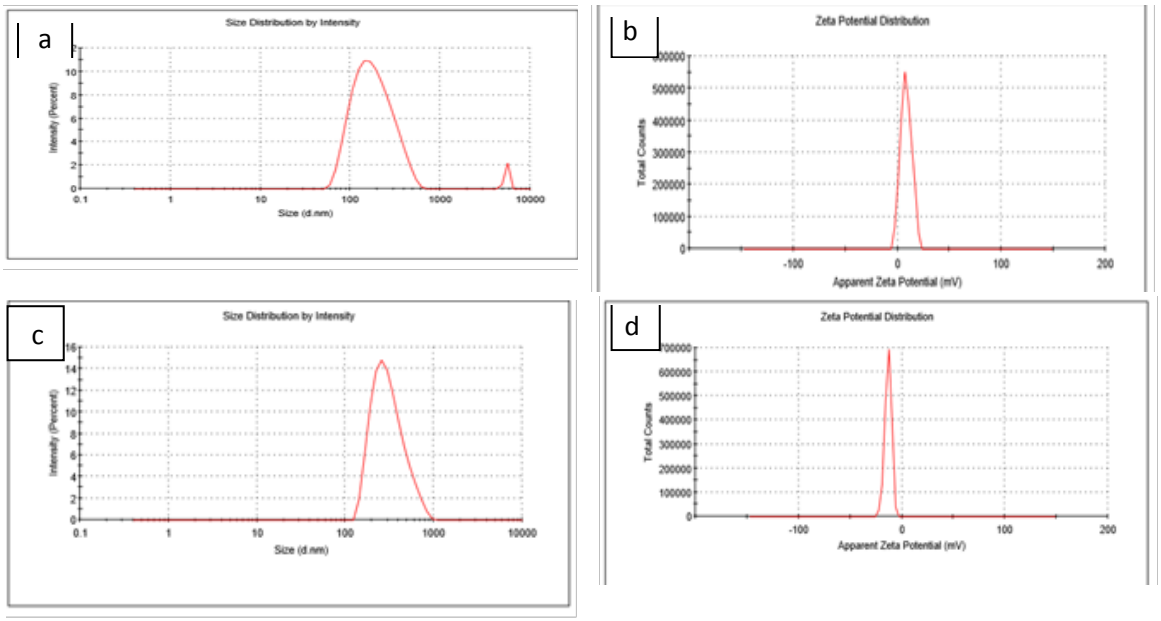

Fig. 5. Zeta average size of (a) Mg-Al (c) Mg-Al oxytetracycline layered double hydroxide, Zeta potential of (b) Mg-Al (d) Mg-Al oxytetracycline LDH.

TABLE 1. **Zeta potential of Mg-Al LDH before and after adsorption with oxytetracycline.**

Zeta values	Mg-Al LDH	Mg-Al oxytetracycline LDH
Zeta potential	8.3	-13.3
Zeta Average	193.3	318.9

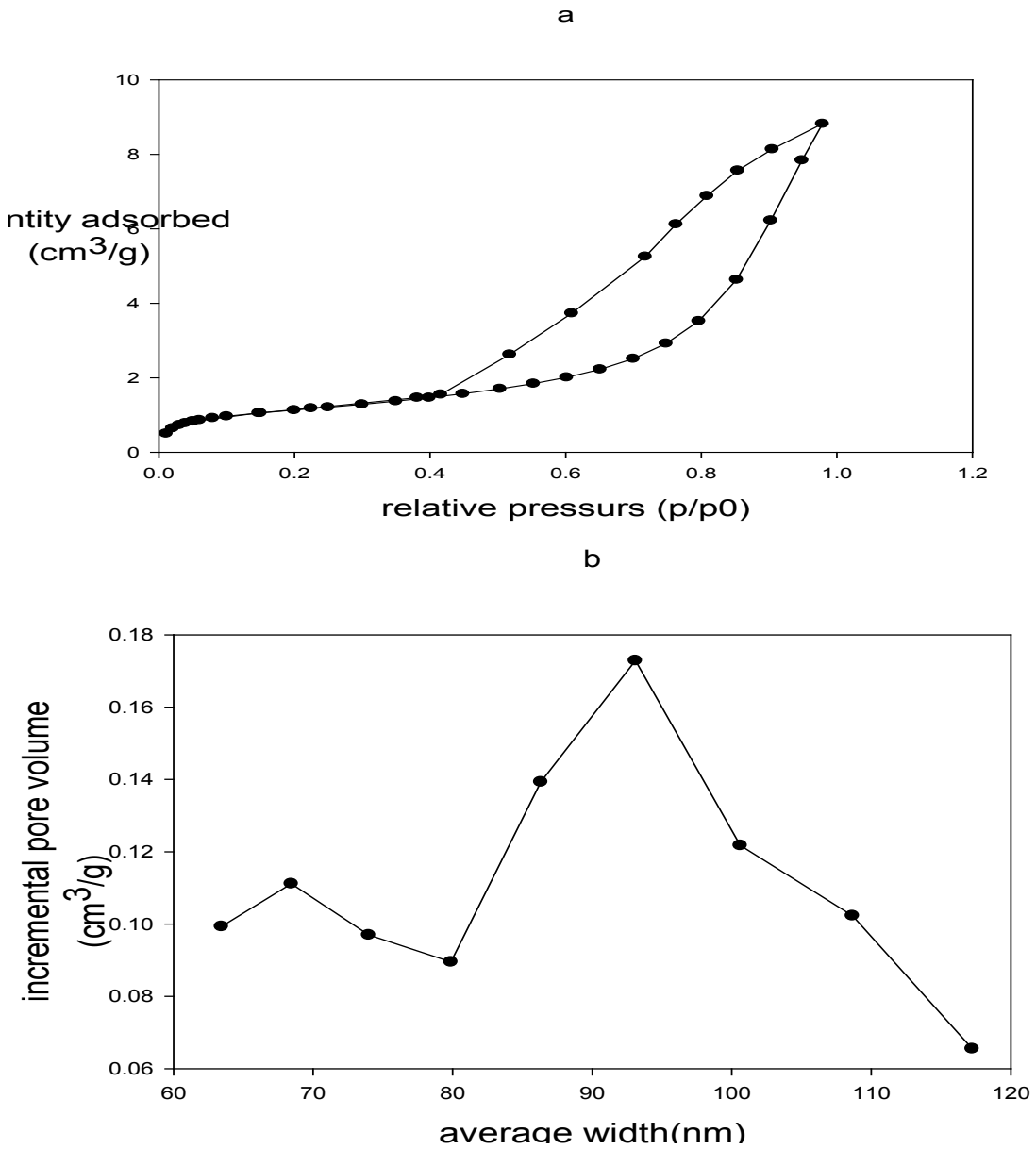

Fig.6. (a). N2 sorption isotherms and (b) pore size distribution of Mg-Al LDH.

TABLE 2. Surface area measurements for Mg-Al LDH.

Surface area (m^2/g)	4.0184
Total pore volume (cc/g)	0.0059
Average pore diameter(nm)	64.167
Micro pore volume (cc/g)	0.001351

precipitating agent NaOH which was used in the synthesis of LDH; that is why hardly micro and mesopores have been found in synthesized LDH [60]. In Figure 6 (b) the pore size distribution of Mg-Al LDH showed two peaks. The wide distribution of pore size in figure (6) b (60-120 nm, maximum at 93.107 nm) for Mg-Al LDH, is due to agglomeration of particles. The specific surface area, total pore volume and average pore size, diameter and micro pore volume were listed in Table 2.

Adsorption studies

Influence of initial pH on the adsorption of pollutants in single contaminated system.

In order to give more information about the adsorption process, the effect of pH on the adsorption of heavy metals under investigation was performed. The pH value is the most important factor that affects on heavy metal ions adsorption, and the medium affecting the metal speciation and toxicity. Thus, at acidic medium more protons saturate metal binding sites, while at basic conditions, metal ions exchange protons to produce other species such as hydroxo-metal complexes. Some of the hydroxo-metal complexes are soluble in water and the others are not, but some of them are toxic soluble in water as mono hydroxo complex species formed by Cd^{2+} ion, so toxicity increases by increasing the pH and cells adsorb more of metal ions under this conditions. However, at high acidic conditions, three cases might occur, firstly, metals compete with protons for binding sites on the surface of the cell. Secondly, different functional groups are protonated leading to reduction of the attraction between metal cations and the membrane. Thirdly, removing the metal from the cell by efflux pumps that was done by proton motive force [49]. The pH value of the Mg/Al LDH adsorbent was around 7.0 as shown in Fig. 7. It was suggested that the heavy metals adsorption capacity increased gradually with pH increase below pH 7.0 and then decreased sharply with pH increase. As shown in Fig.7 the high adsorpitivity of Mg-Al LDH to oxytetracycline at pH 7 was due to the dissociation constant; this phenomenon may be

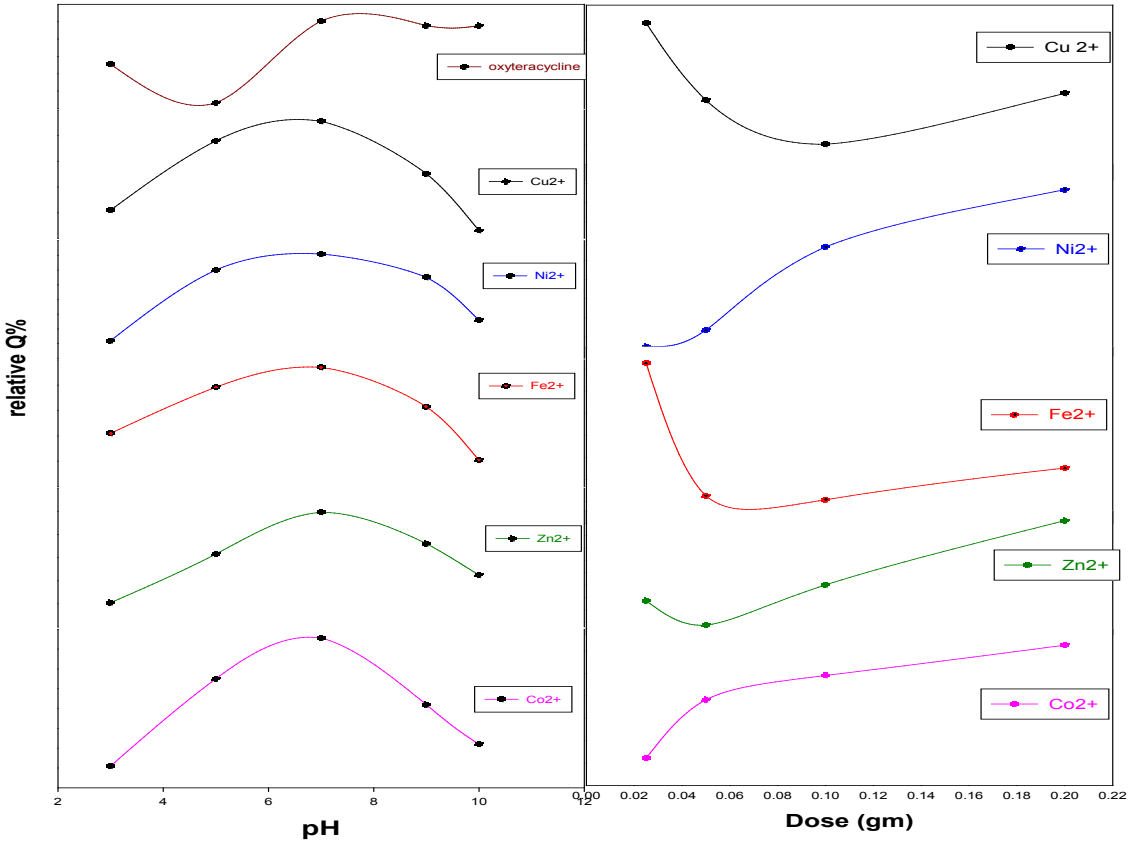

Fig. 7. Effect of different pH on the adsorption of oxytetracycline and metal ions (Cu2+, Ni2+, Co2+, Fe2+ and Zn2+) in single solution and effect of dose of Mg-Al LDH on the adsorption of metal ions (Cu2+, Ni2+, Co2+, Fe2+ and Zn2+)in single solution.

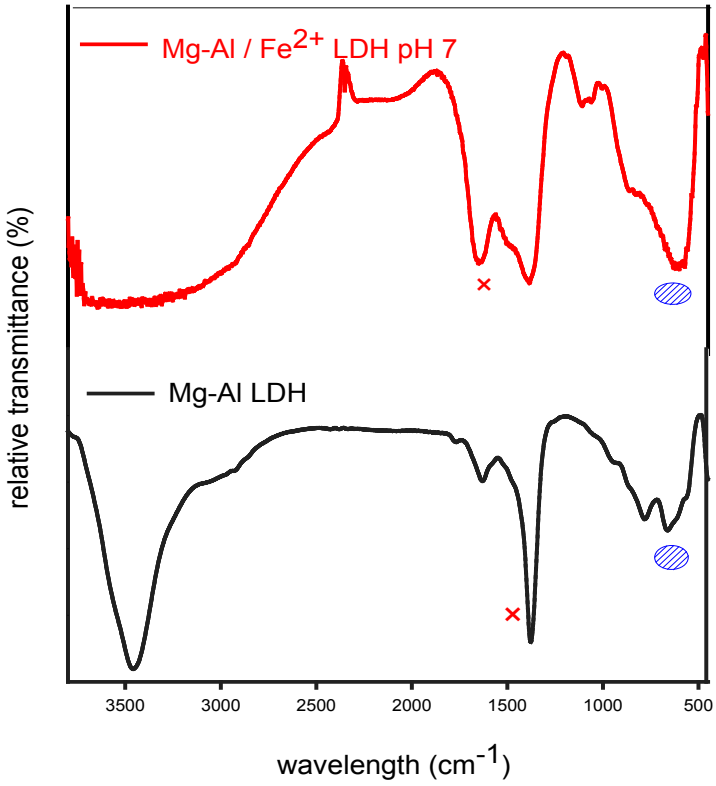

Fig.8. FT-IR spectra of Mg-Al layered double hydroxide after adsorption with iron at different pH in single solution.

related to the ability of oxytetracycline to form high stable complexes with Mg and Al (stability constant ($\log k^{Mg}_{Mg-Oxy}$)of binary complex with respect to oxytetracycline with Mg is 28.74 [61] .

As shown in Fig.8, there is a change in the FTIR chart after adsorption with iron at pH 7, which is taken as a representative example. This may be attributed to that Mg-Al LDH has adsorbed high percentage of the antibiotic.

Effect of dose of Mg-Al LDH on the adsorption of pollutants in single contaminated system.

As indicated in Fig. 7, the adsorption of pollutants increases with the increase of the initial adsorbents dose in case of Ni^{2+} and Co^{2+} metal ions; this may be attributed to the increase in the driving force from the active sites where in case of Cu^{2+} and Fe^{2+} the pollutants adsorption decreases with the increase of adsorbent dose then still constant and in case of Zn^{2+} there is a little decrease in the adsorption then pollutant adsorption increases with the increase of adsorbent dose.

Isotherm studies

There was an increase in the adsorption abilities of Mg-Al LDH toward pollutants with increase in contaminants concentration to a certain limit, and then any further increase in concentration leads to decrease in adsorpitivity as shown in Table 3. As the concentration of metal ions in waste water is about 15 mg/L [62], the concentration of tested metal ions was 20 mg/L, such a concentration is higher than the main concentration of metal ions in waste water and this helped to test the efficiency of Mg-Al LDH. The equilibrium adsorption isotherms are significant for deciding the adsorption capacity of pollutants and detecting the nature of adsorption onto the LDH adsorbent. The equilibrium adsorption potential of the adsorbent was investigated by equation 2, where C_e was assessed for first concentration of each ion which ranges from 10 to 60 mg/L after equilibrium time. Figures 9 and 10 display the adsorption isotherms of Cu^{2+}, Ni^{2+}, Co^{2+}, Zn^{2+} and Fe^{2+} ions

TABLE 3. Isotherm parameters for removal of harmful metal ions by Mg-Al LDH.

Isotherms	Parameters	Cu^{2+}	Ni^{2+}	Co^{2+}	Zn^{2+}	Fe^{2+}
	q_0 (mg/g)	5.605	3.1	6.265	5.546	5.75
Langmuir	K_L (l/mg)	297.61	370.37	270.27	225.73	196.07
	R^2	0.9992	0.9998	0.9994	0.9991	0.9987
	K_F	5.521	3.015	6.243	5.527	5.744
	1/n	0.0104	0.0228	0.0121	0.0157	0.0135
Freundlich	R^2	0.8511	0.901	0.8399	0.8505	0.8128

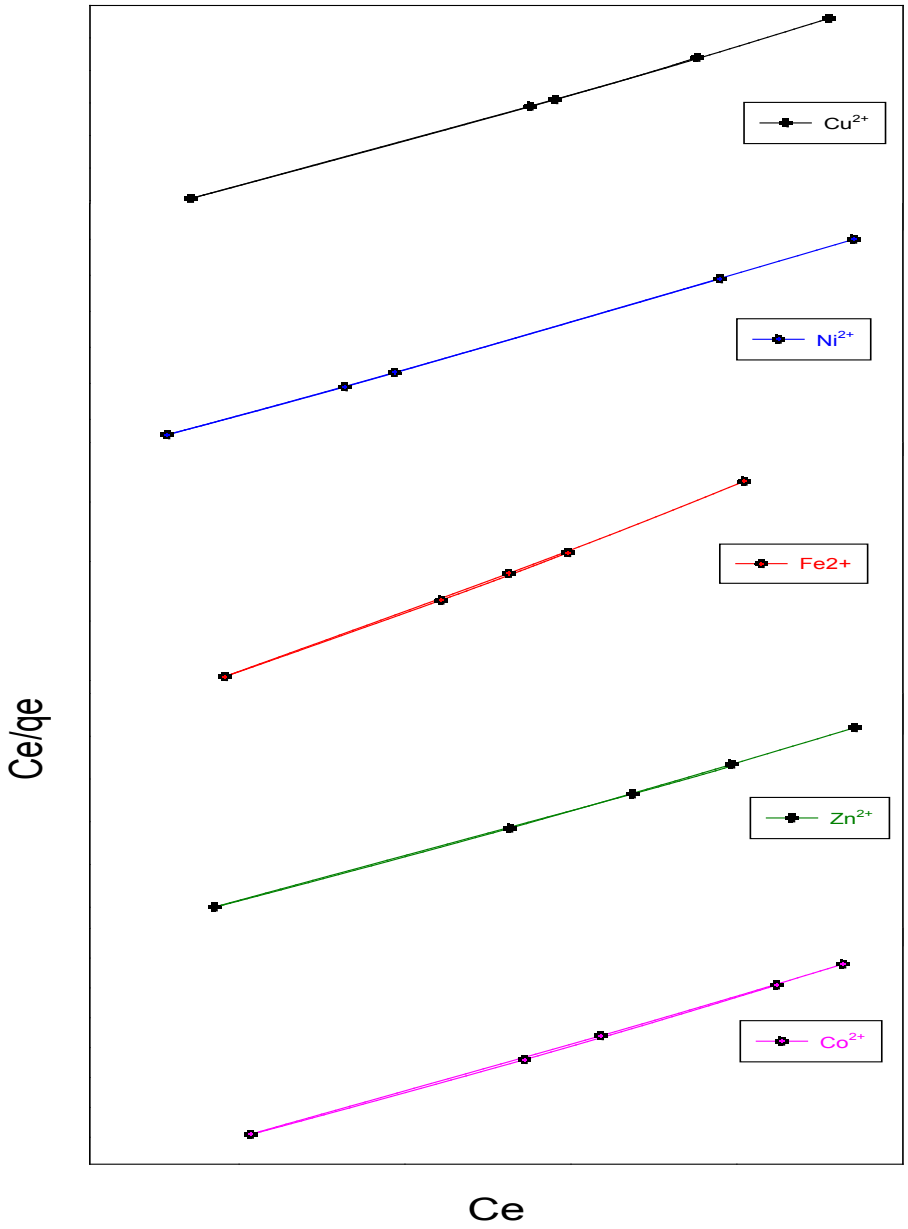

Fig. 9. Adsorption isotherm of Cu2+, Ni2+, Co2+, Zn2+ and Fe2+ ions in single solution on Mg-Al LDH (Langmuir isotherms).

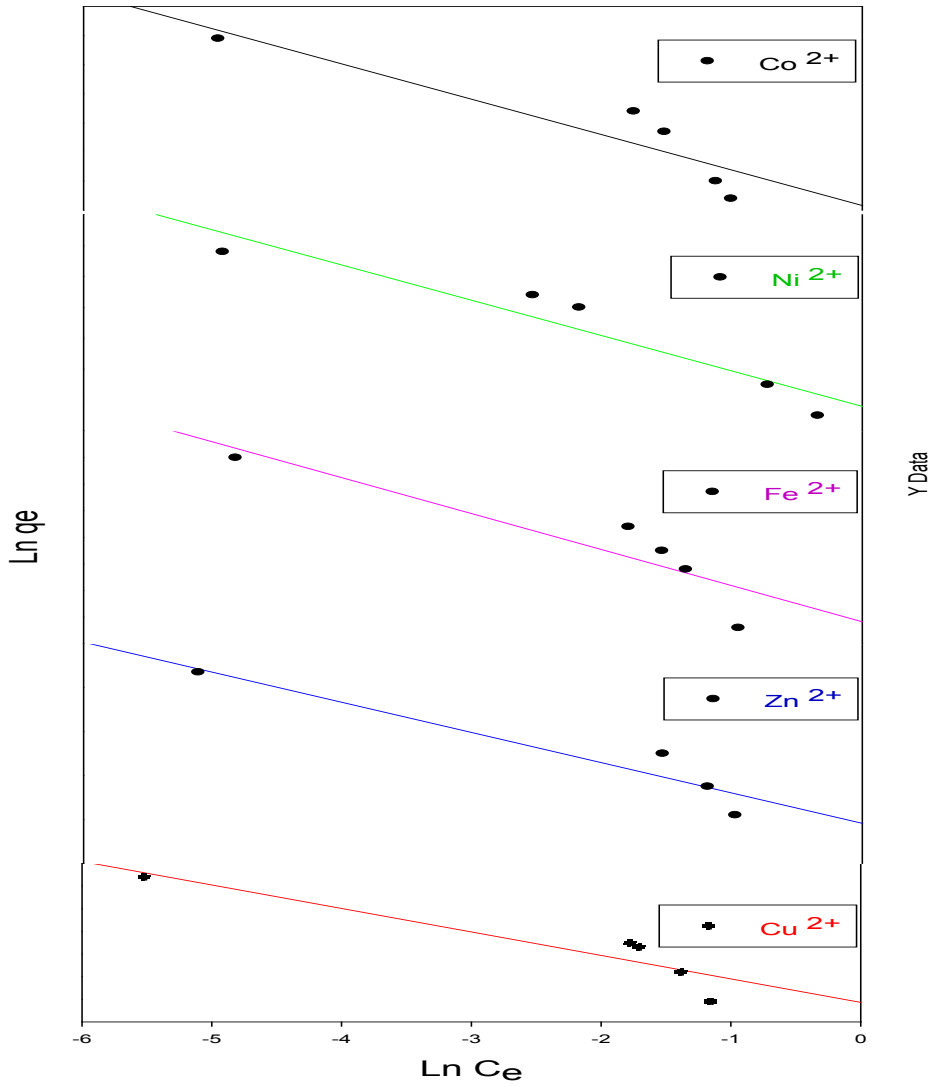

Fig.10. Adsorption isotherm of Cu2+, Ni2+, Co2+, Zn2+ and Fe2+ ions in single solution on Mg-Al LDH (Freundlich isotherm)

respectively, on Mg-Al LDH. Furthermore, these figures show that most widespread models used to investigate the adsorption isotherm are Langmuir and Freundlich models. The Langmuir adsorption isotherm was employed to equilibrium adsorption assuming monolayer adsorption onto a surface with a finite number of identical sites, as illustrated by the equation [52, 63, 64].

$$\frac{C_e}{q_e} = \frac{1}{(q_0 K_L)} + \frac{1}{q_0} C_e \qquad (3)$$

Where C_e (mg/L) is the equilibrium concentration, q_e (mg/g) is the amount of adsorbate adsorbed/unit mass of adsorbate, and q_o (mg/g) and K_L are the Langmuir constants related to the adsorption capacity and the rate of adsorption, respectively. Plotting C_e/q_e against C_e showed a straight line with a slope of $1/q_e$. The Langmuir constants K_L and q_o were determined from this isotherm. The Freundlich model of isotherm is an experimental equation utilized for describing the multilayer adsorption with the interaction between the adsorbed molecules ions [52, 63, 64]. The linear form of Freundlich adsorption isotherm takes the following form of (equation 4):

$$lnq_e = lnK_f + (\frac{1}{n})lnC_e \qquad (4)$$

where q_e is the amount adsorbed at equilibrium (mg/g) and C_e is the equilibrium concentration of pollutant ions, K_F and n are

Freundlich constants, where K_F [(mg/g)/(mg/L)1/n] is the adsorption capacity of the adsorbent and n gives an indication of the favorability of the adsorption process. The slope of the linear relation is 1/n and its value is a measure of the adsorption intensity or surface heterogeneity and ranges from 0 to 1. So, the more heterogeneous the surface is, the closer the value is to 0. Furthermore, the plot of ln q_e versus ln C_e provides straight lines with slope 1/n [65].

Influence of time and kinetics of adsorption.

The influence of time on the adsorption of Cu^{2+} onto Mg-Al LDH was shown in Figure 8. It was found that the removal percentage decreased by increasing the contact time to reach about 99.51% after 120 min. The kinetics of adsorption is an important aspect of the Cu^{2+} removal process control. By applying kinetic models and studying the rate-controlling mechanism, parameters such as mass transfer, chemical reaction, and diffusion control could be explained. To examine the mechanisms of the pollutant adsorption process, the linear equations of the three kinetic models were applied as shown in Figure 11. The pseudo-first-order model suggested that the binding generated from physical adsorption and is interpreted by equation 5. The pseudo second-order model is rooted in chemical adsorption (chemisorptions) and presented by equation 6. In addition, the kinetic results were analyzed, using the intra-particle diffusion model, to explain the diffusion mechanism (equation 7):

$$\ln(q_{e-} q_t) = \ln(q_e) - k_1 t \quad (5)$$

$$\frac{t}{q} = \frac{1}{k_2 q_e^2} + \frac{t}{q_e} \quad (6)$$

$$q_t = k_i t^{0.5} + C \quad (7)$$

In the equations, q_t and q_e are considered the amounts of Cu^{2+} adsorbed on the Mg-Al LDH adsorbent in mg (adsorbate)/g (adsorbent) at time t and at equilibrium, respectively, k_1 is regarded the rate constant of the pseudo first-order model (min^{-1}).

Table 4 summarizes the coefficients of the models. Comparing the regression coefficients for each expression, the results displayed that both the first order rate expression and the intra-particle diffusion model are completely valid for the present system. This is could be explained by the high correlation coefficients in the two types of LDH. On the other hand, the second order kinetic model did not show a good fit of goodness to the experimental data as illustrated by the adsorbate in Figure 11. Also, using the pseudo-fist order model for the linear plots, it shows strong correlation coefficients (in most cases >0.99). This assures that both the theoretical and experimental q_e values agree with each others. Consequently, this provides an indication that the sorption of Cu^{2+} in single solutions by Mg/Fe LDH catalyst is controlled kinetically by the first order reaction compared to the second order process that asserted physical adsorption.

Conclusion

Mg–Al LDH nanoparticles with nitrate intercalated anions was prepared through coprecipitation technique and was used as an adsorbent for some pollutants in wastewater like (copper, zinc, iron, cobalt, nickel metal ions and oxytetracycline) in single solution. This nanomaterial was characterized before and after the adsorption process by XRD, FT-IR, BET surface area, zeta potential, FESEM and HRTEM. To

TABLE 4. Coefficients of the pseudo-first-order and second-order adsorption kinetic models and intraparticle diffusion model (Cu^{2+}=20 ppm, Mg-Al-LDH 0.05 g).

Order models	Parameters	Cu^{2+}
Pseudo-first-order	q_e (mg/g)	1.135
	K_1 (min^{-1})	0.029
	R^2	0.693
Pseudo-second-order	q_e (mg/g)	0.0899
	K_2 (g/mg min)	0.1712
	R^2	1
Intraparticle diffusion model	k_i (mg/g $min^{0.5}$)	
	C (mg/g)	5.2183
	R^2	0.929

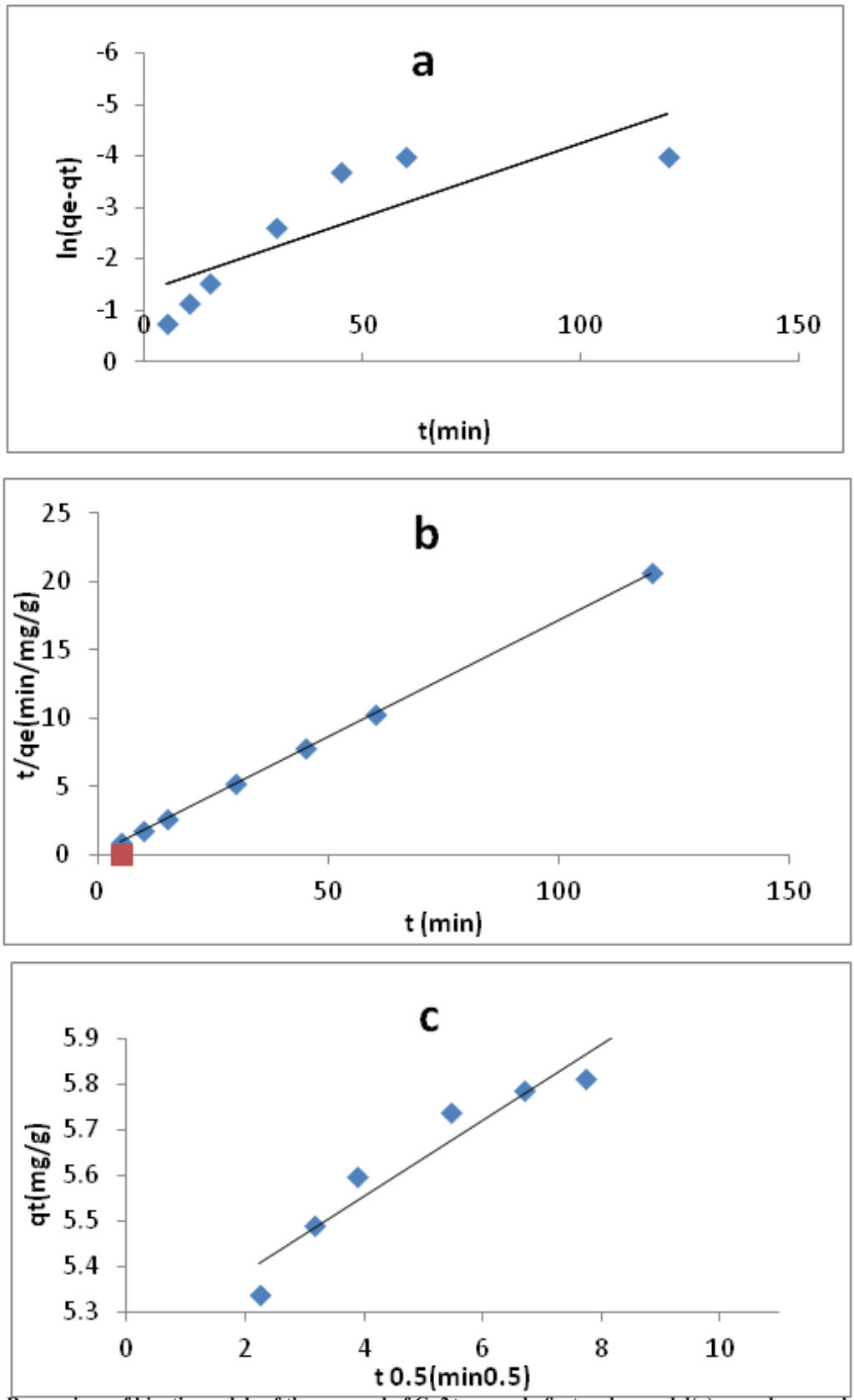

Fig. 11. Regressions of kinetic models of the removal of Cu2+ ; pseudo first-order model(a), pseudo second-order model (b), and intraparticle diffusion model (c).

optimize the removal ability of Mg-Al LDH, the factors affecting the process such as pH, dose of Mg-Al LDH, concentration of metal ions and effect of shaking time have been studied, and the sorption kinetics for heavy metal ions follow a pseudo-first order model. The microstructures of LDH samples were uniform in nature with porous nano sheets with a thickness of about 5-45 nm and composed of plate-like nanoparticles. The adsorption isotherm was investigated with Langmuir and Freundlich models, and the adsorption experimental results of heavy metal ions were fitted by the Langmiur adsorption one. In addition, the efficient removal of oxytetracycline and some heavy metal ions from aqueous solutions by Mg-Al layered double hydroxide nanomaterial has amounted to 60% and 99%, respectively.

Conflicts of interest

The authors declare that they haven't conflict of interest.

References

1. Klaver A.L. and Matthews R.A. Effects of oxytetracycline on nitrification in a model aquatic system. *Aquaculture*, **123**: 237-47 (1994).
2. Martinez J.L. Environmental pollution by antibiotics and by antibiotic resistance determinants. *Environmental Pollution*, **157**: 2893-902 (2009).
3. Taylor H. and Lijnsky W. Tumor induction in rats by feeding aminopyrine or oxytetracycline with nitrite. *International Journal Of Cancer*, **16**: 211-5 (1975).
4. Sponza DT and Çelebi H. Removal of oxytetracycline (OTC) in a synthetic pharmaceutical wastewater by sequential anaerobic multichamber bed reactor (AMCBR)/ completely stirred tank reactor (CSTR) system: biodegradation and inhibition kinetics. *Journal of Chemical Technology & Biotechnology*, **87**: 961-75 (2012).
5. Kadirvelu K., Thamaraiselvi K. and Namasivayam C. Removal of heavy metals from industrial wastewaters by adsorption onto activated carbon prepared from an agricultural solid waste. *Bioresource Technology*, **76**: 63-5 (2001).
6. Fu F. and Wang Q. Removal of heavy metal ions from wastewaters: a review. *Journal of environmental management*, **92**: 407-18 (2011).
7. Abd-Elhamid A.I. and Aly H.F. Removal of Fe (III) from Aqueous Solution Using Thiosalcylic Acid as an Efficient and Novel Adsorbent. *Egyptian Journal of Chemistry,* **61**: 617-627 (2018).
8. Simon N. Loosely bound oxytetracycline in riverine sediments from two tributaries of the Chesapeake Bay. *Environmental science & technology*, **39**: 3480-7 (2005).
9. Miao X.S., Bishay F., Chen M. and Metcalfe C.D. Occurrence of antimicrobials in the final effluents of wastewater treatment plants in Canada. *Environmental Science & Technology*, **38**: 3533-41 (2004).
10. Kolpin D.W., Skopec M., Meyer M.T., Furlong E.T. and Zaugg S.D. Urban contribution of pharmaceuticals and other organic wastewater contaminants to streams during differing flow conditions. *Science of the Total Environment*, **328**: 119-30 (2004).
11. Vidaver A.K. Uses of antimicrobials in plant agriculture. *Clinical Infectious Diseases*, 34: S107-S10 (2002).
12. Chi Z., Liu R., Yang B. and Zhang H. Toxic interaction mechanism between oxytetracycline and bovine hemoglobin. *Journal of Hazardous Materials*, **180**: 741-7 (2010).
13. Jaishankar M., Tseten T., Anbalagan N., Mathew B.B. and Beeregowda K.N. Toxicity, mechanism and health effects of some heavy metals. *Interdisciplinary Toxicology*, **7**: 60-72 (2014).
14. Ferreira C.S.G., Nunes B.A., de Melo Henriques-Almeida J.M. and Guilhermino L. Acute toxicity of oxytetracycline and florfenicol to the microalgae Tetraselmis chuii and to the crustacean Artemia parthenogenetica. *Ecotoxicology and Environmental Safety*, **67**: 452-8 (2007).
15. Mohan D. and Singh K.P. Single-and multi-component adsorption of cadmium and zinc using activated carbon derived from bagasse—an agricultural waste. *Water research*, **36**: 2304-18 (2002).
16. Zhao X., Jia Q., Song N., Zhou W. and Li Y. Adsorption of Pb (II) from an aqueous solution by titanium dioxide/carbon nanotube nanocomposites: kinetics, thermodynamics, and isotherms. *Journal of Chemical & Engineering Data,* **55**: 4428-33 (2010).
17. Du W., Yin L., Zhuo Y., Xu Q., Zhang L. and Chen C. Catalytic oxidation and adsorption of elemental mercury over $CuCl_2$-impregnated sorbents. *Industrial & Engineering Chemistry Research*, **53**: 582-91 (2014).

18. Attia A.A., Shouman M.A. and El-Khouly S.M. Insights onto the Adsorption of MFe2O4 Nanoparticles Loaded onto Activated Carbon. *Egyptian Journal of Chemistry*, **60**: 537-49 (2017).

19. Albadarin A.B., Ala'a H., Al-Laqtah N.A., Walker G.M., Allen S.J. and Ahmad M.N. Biosorption of toxic chromium from aqueous phase by lignin: mechanism, effect of other metal ions and salts. *Chemical Engineering Journal,* **169**: 20-30 (2011).

20. Liu J., Ma Y., Xu T. and Shao G. Preparation of zwitterionic hybrid polymer and its application for the removal of heavy metal ions from water. *Journal of Hazardous Materials,* **178**: 1021-9 (2010).

21. Gode F.and Pehlivan E. Sorption of Cr (III) onto chelating b-DAEG–sporopollenin and CEP–sporopollenin resins. *Bioresource Technology,* **98**: 904-11 (2007).

22. Pyrzyńska K. and Bystrzejewski M. Comparative study of heavy metal ions sorption onto activated carbon, carbon nanotubes, and carbon-encapsulated magnetic nanoparticles. *Colloids and Surfaces A: Physicochemical and Engineering Aspects,* **362**: 102-9 (2010).

23. Ma L., Wang Q., Islam S.M., Liu Y., Ma S. and Kanatzidis M.G. Highly selective and efficient removal of heavy metals by layered double hydroxide intercalated with the MoS_4^{2-}ion. *Journal of the American Chemical Society,* **138**: 2858-66 (2016).

24. Gunatilake S.K. Methods of removing heavy metals from industrial wastewater. *Journal of Multidisciplinary Engineering Science Studies (JMESS)*, **1**: 12-18 (2015).

25. Walha K., Amar R.B., Firdaous L., Quéméneur F. and Jaouen P. Brackish groundwater treatment by nanofiltration, reverse osmosis and electrodialysis in Tunisia: performance and cost comparison. *Desalination*, **207**: 95-106 (2007).

26. Oladipo A.A., Ifebajo A.O, Nisar N. and Ajayi O.A. High-performance magnetic chicken bone-based biochar for efficient removal of rhodamine-B dye and tetracycline: competitive sorption analysis. *Water Science and Technology*, **76**: 373-85 (2017).

27. Babaei A.A., Lima E.C., Takdastan A., Alavi N., Goudarzi G., Vosoughi M., Hassani G. and Shirmardi M. Removal of tetracycline antibiotic from contaminated water media by multi-walled carbon nanotubes: operational variables, kinetics, and equilibrium studies. *Water Science and Technology*, **74** (5): 1202-16 (2016).

28. Li G., Guo Y. and Zhao W. Efficient adsorption removal of tetracycline by layered carbon particles prepared from seaweed biomass. *Environmental Progress & Sustainable Energy*, **36**: 59-65 (2017).

29. Chen Y., Wang F., Duan L., Yang H. and Gao J. Tetracycline adsorption onto rice husk ash, an agricultural waste: its kinetic and thermodynamic studies. *Journal of Molecular Liquids*, **222**: 487-94 (2016).

30. Ifebajo A.O., Oladipo A.A. and Gazi M. Efficient removal of tetracycline by CoO/CuFe 2 O 4 derived from layered double hydroxides. *Environmental Chemistry Letters*, **16**: 1-8 (2018).

31. Almomani F.A., Shawaqfah M., Bhosale R.R. and Kumar A. Removal of emerging pharmaceuticals from wastewater by ozone□based advanced oxidation processes. *Environmental Progress & Sustainable Energy*, **35**: 982-95 (2016).

32. Mishra G., Dash B., Pandey S. Layered double hydroxides: A brief review from fundamentals to application as evolving biomaterials. *Applied Clay Science,* **153**: 172-86 (2018).

33. Mohapatra L. and Parida K. A review on the recent progress, challenges and perspective of layered double hydroxides as promising photocatalysts. *Journal of Materials Chemistry A*, **4**: 10744-66 (2016).

34. Sharma V., Kumar RV., Pakshirajan K. and Pugazhenthi G. Integrated adsorption-membrane filtration process for antibiotic removal from aqueous solution. *Powder Technology*, **321**: 259-69 (2017).

35. Mishra G., Dash B., Sethi D., Pandey S. and Mishra B. Orientation of organic anions in Zn-Al layered double hydroxides with enhanced antibacterial property. *Environmental Engineering Science*, **34**: 516-27 (2017).

36. Zhou H., Jiang Z. and Wei S. 2018. A new hydrotalcite-like absorbent FeMnMg-LDH and its adsorption capacity for Pb^{2+} ions in water. *Applied Clay Science*, **153**: 29-37 (2017).

37. Parida K. and Mohapatra L. Carbonate intercalated Zn/Fe layered double hydroxide: a novel photocatalyst for the enhanced photo degradation of azo dyes. *Chemical Engineering Journal*, **179**:

131-9 (2012).

38. Dou R, Ma J, Huang D, Fan C, Zhao W, et al. Bisulfite assisted photocatalytic degradation of methylene blue by Ni-Fe-Mn oxide from MnO_4^- intercalated LDH. *Applied Clay Science* **161**: 235-41 (2018).

39. Mu'azu N.D., Jarrah N., Kazeem T.S., Zubair M. and Al-Harthi M. Bentonite-layered double hydroxide composite for enhanced aqueous adsorption of Eriochrome Black T. *Applied Clay Science*, **161**: 23-34 (2018).

40. Stawiński W., Węgrzyn A., Mordarski G., Skiba M., Freitas O. and Figueiredo S.A. Sustainable adsorbents formed from by-product of acid activation of vermiculite and leached-vermiculite-LDH hybrids for removal of industrial dyes and metal cations. *Applied Clay Science,* **161**: 6-14 (2018).

41. Meng Z., Wu M., Yu Y., Meng F., Liu A., Sridhar Komarneni S. and Zhang Q. Selective removal of methyl orange and Cr anionic contaminants from mixed wastewater by in-situ formation of Zn-Al layered double hydroxides. *Applied Clay Science*, **161**: 1-5 (2018).

42. Zubair M., Daud M., McKay G., Shehzad F. and Al-Harthi M.A. Recent progress in layered double hydroxides (LDH)-containing hybrids as adsorbents for water remediation. *Applied Clay Science,* **143**: 279-92 (2017).

43. Yuan F., Song C., Sun X., Tan L., Wang Y. and Wang S. Adsorption of Cd (II) from aqueous solution by biogenic selenium nanoparticles. *RSC Advances,* **6**: 15201-9 (2016).

44. Shan R.R.., Yan L.G., Yang K., Hao Y.F. and Du B. Adsorption of Cd (II) by Mg–Al–CO_3^- and magnetic Fe_3O_4/Mg–Al–CO_3^-layered double hydroxides: kinetic, isothermal, thermodynamic and mechanistic studies. *Journal of hazardous materials*, **299**: 42-9 (2015).

45. Shi T., Jia S., Chen Y., Wen Y., Du C., Guo H. and Wang Z. Adsorption of Pb (II), Cr (III), Cu (II), Cd (II) and Ni (II) onto a vanadium mine tailing from aqueous solution. *Journal of hazardous materials*, **169**: 838-46 (2009).

46. Sun W., Jiang B., Wang F. and Xu N. Effect of carbon nanotubes on Cd (II) adsorption by sediments. *Chemical Engineering Journal*, **264**: 645-53 (2015).

47. Balcomb B., Singh M. and Singh S. Synthesis and characterization of layered double hydroxides and their potential as nonviral gene delivery vehicles. *Chemistry Open*, **4**: 137-45 (2015).

48. Yu H., Park J., Lee K., Yoon J., Kim K., et al. 2015. Recent advances in wavefront shaping techniques for biomedical applications. *Current Applied Physics*, **15**: 632-41 (2015).

49. Moaty S.A., Farghali A. and Khaled R. Preparation, characterization and antimicrobial applications of Zn-Fe LDH against MRSA. *Materials Science and Engineering: C*, **68**: 184-93 (2016).

50. Meng Z., Zhang Y., Zhang Q., Chen X., Liu L., Komarneni S. and Lv F. Novel synthesis of layered double hydroxides (LDHs) from zinc hydroxide. A*pplied Surface Science*, **396**: 799-803 (2017).

51. Moriyama S., Sasaki K. and Hirajima T. Effect of freeze drying on characteristics of Mg–Al layered double hydroxides and bimetallic oxide synthesis and implications for fluoride sorption. *Applied Clay Science*, **132**: 460-7 (2016).

52. Araújo C.S., Almeida I.L., Rezende H.C., Marcionilio S.M., Léon J.J. and de Matos T.N. Elucidation of mechanism involved in adsorption of Pb (II) onto lobeira fruit (Solanum lycocarpum) using Langmuir, Freundlich and Temkin isotherms. *Microchemical Journal*, **137**: 348- 54 (2018).

53. Ahmed I. and Gasser M. Adsorption study of anionic reactive dye from aqueous solution to Mg–Fe–CO_3 layered double hydroxide (LDH). *Applied Surface Science*, **259**: 650-6 (2012).

54. Chen M.L. and An M.I. Selenium adsorption and speciation with Mg–$FeCO_3$ layered double hydroxides loaded cellulose fibre. *Talanta*, **95**: 31-5 (2012).

55. Abdelkader N.B.H., Bentouami A., Derriche Z., Bettahar N. and De Menorval L.C. Synthesis and characterization of Mg–Fe layer double hydroxides and its application on adsorption of Orange G from aqueous solution. *Chemical Engineering Journal*, **169**: 231-8 (2011).

56. Hernandez-Moreno M.J., Ulibarri M.A., Rendon J. and Serna C.J. IR characteristics of hydrotalcite-like compounds. *Physics and Chemistry of Minerals*, **12**: 34-8 (1985).

57. Lv L., He J., Wei M., Evans D. and Duan X. Factors influencing the removal of fluoride from aqueous

solution by calcined Mg–Al–CO_3 layered double hydroxides. *Journal of Hazardous Materials*, **133**: 119-28 (2006).

58. Kang D., Yu X., Tong S., Ge M., Zuo J., Cao C. and Song W. Performance and mechanism of Mg/Fe layered double hydroxides for fluoride and arsenate removal from aqueous solution. *Chemical Engineering Journal*, **228**: 731-40 (2013).

59. Katanić-Popović J., Miljević N. and Zec S. Spinal formation from coprecipitated gel. *Ceramics International*, **17**: 49-52 (1991).

60. Labrecque G., Doré F.M., Bélanger P.M. and Carter V. Chronobiological study of plasma exudation in carrageenan-paw oedema in the rat. *Agents and Actions*, **14**: 719-22 (1984).

61. Wahed K.A.E., Ayad M. and Sheikh R.E. Potentiometric study of tetracycline and oxytetracycline with some metal ions of biological interest. *Analytical letters*, **17**: 413-22 (1984).

62. Dean J.G., Bosqui F.L. and Lanouette K.H. Removing heavy metals from waste water. *Environmental Science & Technology*, **6**: 518-22 (1972).

63. Asci B., Kovenc E., Arar O. and Arda M. Kinetic, isotherm and thermodynamic investigations of nitrite (NO_2^-) removal from water by anion exchange resins. *Global Nest Journal*, **20**: 368-72 (2018).

64. Alyüz B. and Veli S. Kinetics and equilibrium studies for the removal of nickel and zinc from aqueous solutions by ion exchange resins. *Journal of Hazardous Materials*, **167**: 482-8 (2009).

65. Li X., Cao W.C., Liu Y.G., Zeng G.M., Zeng W., Qin L.and Li T. T. Property variation of magnetic mesoporous carbon modified by aminated hollow magnetic nanospheres: synthesis, characterization, and sorption. *ACS Sustainable Chemistry & Engineering*, **5**: 179-88 (2016).